

A UNIVERSAL REDUCED DAMPING PARAMETER FOR PREDICTION OF VORTEX-INDUCED VIBRATION

J. Kim Vandiver
Massachusetts Institute of Technology

ABSTRACT

A dimensionless parameter, S_u , is proposed which enables a clear presentation of vortex-induced vibration response data in sheared and uniform flows. The ability of the parameter to account for the effects of damping, flow velocity and power-in length is demonstrated with response data from an unusual set of experiments conducted by SHELL Development Co. The historical relationship of the new parameter to the earlier work of Owen Griffin is also presented.

Key words: Vortex-induced vibration, reduced damping

INTRODUCTION

At the present time there is no dimensionless parameter in use, which allows systematic organization and understanding of cross-flow VIV response amplitude in a sheared flow. Such a parameter is needed to guide engineers in making response estimates for a broad variety of design problems and in the calibration and verification of empirically-based response prediction programs such as SHEAR7[Vandiver & Lee, 2002].

The parameter introduced in this paper is a variation of the response parameter, S_g , described Skop and Griffin, 1975. To date, S_g has been used only for uniform flows. The new parameter is called S_u , with the subscript 'u' for 'universal' signifying the usefulness of the parameter for a wide variety of uniform and non-uniform flow conditions. Once sufficient measured data are cataloged in terms of this parameter, it will be possible to estimate the upper bound modal response of flexible cylinders in a variety of sheared profiles, by referring to graphs of A/D versus S_u .

NOMENCLATURE

A/D amplitude to diameter ratio
 $C_a, \overline{C_a}$ add mass coefficient & its spatial average
 $C_L(x)$ lift coefficient
 $\langle C_{L,n} \rangle$ modal average lift coefficient

f_n natural frequency in Hz.
 $f_{v,2}$ observed 2nd mode vibration frequency
 h water depth
 $I_i^{1/2}$ Griffin's mode correction factor
 $L_{in}, L_{out}, \& L$ Power-in, power-out and total lengths
 m_r mass ratio
 m_t total mass per unit length
 m_e Griffin's effective mass/length
 $m(x)$ mass per unit length
 M_n, R_n, K_n modal mass, damping, & stiffness
 n mode number
 $Q_n(t)$ modal force
 $q_n(t)$ mode participation factor
 $r(x)$ damping force/length/velocity
 $R_{h,n}$ hydrodynamic modal damping constant
 $R_{e,\omega}$ vibration Reynolds number
 S_t Strouhal number
 S_g response parameter
 S_u universal reduced damping parameter
 $U(x)$ flow velocity
 U_n average flow velocity in the nth mode power-in zone
 $V_R, \Delta V_R$ Reduced velocity, and reduced velocity bandwidth
 $y(x)$ response amplitude
 Y Peak cylinder response amplitude
 Y_{EFF}/D Griffin's A/D corrected for mode shape
 δ_r reduced damping, Scruton number
 $\psi_n(x)$ mode shape of mode n
 $\rho_f \& \rho_s$ fluid and structural density
 $n\zeta_n$ wave propagation parameter
 ω_n natural frequency in radians/second

DERIVATION OF S_U FOR STANDING WAVE VIBRATION IN A SHEARED OR UNIFORM FLOW

The equation of motion: To begin, consider a flexible cylinder, such as a production riser, in a sheared flow. For this case it is assumed that the product of the mode number and the modal damping, $n\zeta_n$, is assumed to be small (order of 0.2 or less) and that the techniques of mode superposition analysis are valid. Small values of $n\zeta_n$ imply that when the response is dominated by a single resonant mode, pronounced standing wave behavior is observed[Vandiver, 1993].

By the method of modal analysis, the response of one mode at a time may be modeled with an equivalent single degree of freedom model, as follows.

$$M_n \ddot{q}_n + R_n \dot{q}_n + K_n q_n = Q_n(t) \quad (1.1)$$

where

$q_n(t)$ is the modal amplitude for mode n .

$Q_n(t)$ is the modal force. M_n , R_n and K_n are the modal mass, damping, and stiffness coefficients.

$$\omega_n = \sqrt{\frac{K_n}{M_n}}, \text{ and } \zeta_n = \frac{R_n}{2\omega_n M_n}, \text{ are the} \quad (1.2)$$

natural frequency and modal damping ratio. The modal exciting force is assumed to come from periodic vortex shedding on a region of the riser where the shedding frequency and the natural frequency of mode n correspond. This region is known as the power-in region for mode n and has a length L_{in} . Under ideal conditions, this would be called a lock-in region.

Because the excitation is periodic it may be represented by a Fourier series. The first harmonic term of the series is by far the largest and is the term responsible for the resonant excitation and wake synchronization at the natural frequency of the riser. Higher harmonic terms exist (especially the third harmonic) and at times lead to some observable response. These are neglected in the following analysis.

A lift force excitation model The riser is assumed to respond resonantly to this harmonic excitation. At resonance the mass and stiffness terms in the equation of motion cancel, requiring the damping force to be in dynamic equilibrium with the excitation, as stated below.

$$R_n \dot{q}_n = Q_n \cos(\omega_n t) \quad (1.3)$$

where Q_n is assume to be a real and positive.

The solution for $q_n(t)$ is

$$q_n(t) = q_n \sin(\omega_n t) \text{ and therefore} \quad (1.4)$$

$$\dot{q}_n(t) = q_n \omega_n \cos(\omega_n t),$$

where q_n is the magnitude of the modal amplitude.

$Q_n(t)$ is the modal force and comes from lift forces in the power-in region as defined below.

$$Q_n(t) = \frac{1}{2} \rho_f U_n^2 D \cos(\omega_n t) \int_{L_{in}} C_{L,n}(q_n, V_R, x) \psi_n(x) dx$$

$$= \frac{1}{2} \rho_f U_n^2 D L_{in} \langle C_{L,n} \rangle \cos(\omega_n t) \quad (1.5)$$

Where $\langle C_{L,n} \rangle$ is the spatially averaged value of the product of the local lift coefficient, $C_{L,n}(q_n, V_R, x)$, and the mode shape, $\psi_n(x)$. The local lift coefficient is a complex function of response amplitude, reduced velocity, roughness and Reynolds number, and is generally unknown in experiments in which free vibration response is measured. It is represented here as an average over the length of the power-in region.

$$\langle C_{L,n} \rangle = \frac{1}{L_{in}} \int_{L_{in}} C_{L,n}(q_n, V_R, x) \psi_n(x) dx \quad (1.6)$$

The product of the length of the power-in region and this average lift coefficient, $L_{in}^* \langle C_{L,n} \rangle$, is the total modal lift coefficient. ρ_f , U_n , and D are the density of the fluid, the average local flow velocity in the power-in region and the diameter, respectively.

The significance of added mass and reduced velocity

U_n is the velocity which results in coincidence of the shedding frequency and the natural frequency and leads to ideal lock-in conditions. For the purpose of this analysis the average flow velocity within the power-in band is assumed to be U_n . Within a power-in region the allowable variation in the local flow velocity, U , is controlled by the tolerance of the local wake synchronization process to variations in the local reduced velocity, $U/f_n D$. Although there is some variation of the flow velocity within the power-in region, the U^2 term is assumed to be approximately constant with value U_n^2 and is moved outside of the integral in equation(1.5). This is assumed to be sufficiently accurate for the analysis considered here.

The natural frequency, f_n , for any given case being evaluated is fixed. Added mass is a function of reduced velocity. For a given sheared profile the reduced velocity distribution along the riser is fixed at each vibration frequency and therefore the added mass distribution and each natural frequency are fixed. If the flow profile changes, the added mass distribution and natural frequencies may change[Vandiver 2000].

A common conceptual trap must be avoided. In uniform flow experiments on flexible or spring mounted cylinders, it is common to plot response A/D versus the reduced velocity, $V_r = U/f_n D$, where f_n is taken to be a fixed value such as that measured in still water. For low mass ratio cylinders the resulting plot of response, A/D, versus V_r may be very broad, due to the increase of the actual natural frequency with increased V_r . Of course the rise in natural frequency is

associated with the drop in added mass. This rise in natural frequency does not happen due to a change over distance of the inflow velocity. There is only one natural frequency in effect for each mode for each velocity profile.

In the context of this paper the reduced velocity, $V_R = U/f_n D$, is defined using the vibration response frequency, which for each power-in region is a single, fixed f_n . The allowed variation of the reduced velocity within each lock-in region is not a function of mass ratio, but a function only of the ability of the wake to synchronize with the motion of the cylinder. Due to the effects of shear on coherence length the maximum allowable variation in flow velocity and therefore reduced velocity within a lock-in region is expected to be only about 30 to 40%. It is likely to be less than the lock-in range observed in uniform flow, forced, vibration tests. At sub-critical Reynolds numbers lock-in occurs in uniform flows over a reduced velocity range of about 4 to 8, for reduced velocity defined using the actual vibration frequency.

Modal damping evaluation An expression for modal damping, R_n , is also needed.

$$R_n = \int_0^L r(x) \psi_n^2(x) dx \quad (1.7)$$

Where $r(x)$ is the damping force per unit length per unit velocity. It may have structural and hydrodynamic components. Combining the results of equations (1.3) to (1.5) and the assumptions described above leads to:

$$R_n \omega_n q_n = \frac{\langle C_{L,n} \rangle}{2} \rho_f U_n^2 L_{in} D \quad (1.9)$$

The $\cos(\omega_n t)$ terms have cancelled out leaving the statement that the magnitude of the modal damping force equals the modal exciting force.

The solution for S_u Solving for $\frac{q_n}{D}$ yields:

$$\frac{q_n}{D} = \frac{\langle C_{L,n} \rangle}{2} \frac{\rho_f U_n^2 L_{in}}{R_n \omega_n} = \frac{\langle C_{L,n} \rangle}{2 S_u} \quad (1.10)$$

$$\text{where } S_u \equiv \frac{R_n \omega_n}{\rho_f U_n^2 L_{in}} \quad (1.11)$$

This is the fundamental definition of S_u . It is a statement of dynamic equilibrium between modal exciting forces and modal damping forces and explicitly accounts for the length of the power-in region for the mode. It is not a function of the mass per unit length of the cylinder and it is a function of the flow velocity in the power-in region. It is closely related to Griffin's response parameter, S_G , but is different from the Scruton

number [Scruton, 1963], also called the reduced damping [Iwan & Blevins, 1974].

A second formulation for S_u Equation (1.11) is the general definition of S_u , valid for flexible and rigid cylinders with non-time-varying properties. It is useful to have two alternative forms of S_u in terms of quantities such as mass ratio and modal damping ratio. These are briefly derived here. First from equation 1.2 we may express the modal damping as

$$R_n = 2 \omega_n M_n \zeta_n \quad (1.12)$$

Second, a reduced velocity, V_R , may be defined as

$$V_R = \frac{U_n}{f_n D} = \frac{2\pi U_n}{\omega_n D}, \text{ where } f_n \text{ is} \quad (1.13)$$

in Hz and ω_n is in radians/second.

This reduced velocity is intended to be based on the actual vibration frequency observed under lock-in conditions and is not to be based on an arbitrarily defined fixed natural frequency, taken, for example, in still water. Equation (1.13) may be solved for U_n .

$$U_n = \frac{\omega_n D V_R}{2\pi} \quad (1.14)$$

Both equations (1.12) and (1.14) may be substituted into equation (1.11). The result simplifies to a second useful form for the parameter S_u .

$$S_u = \frac{8\pi^2 M_n \zeta_n}{\rho_f D^2 L_{in} V_R^2} \quad (1.15)$$

For those who would rather think in terms of an effective Strouhal number, which for this purpose is define as

$$S_t = 1/V_R, \quad (1.16)$$

then equation (1.15) can be expressed as follows:

$$S_u = \frac{8\pi^2 S_t^2 M_n \zeta_n}{\rho_f D^2 L_{in}} \quad (1.17)$$

The third useful form of the parameter requires a discussion of the historical roots of the reduced damping.

Relating S_u to the historical form of S_G To show how the expressions for S_u , given above, relate to the historical uses of the parameter S_G , it is necessary to derive a third form of S_u , in terms of the quantity known as the mass ratio. Mass ratio has no consistent symbol in the literature. It will be called m_t in this paper.

$$m_t = \frac{m_t}{\rho_f D^2} = \frac{\pi}{4} \left(\frac{\rho_s}{\rho_f} + C_a \right), \text{ where } \rho_f \quad (1.18)$$

and ρ_s are the fluid and structure densities.

m_t is the total mass per unit length including the structural and added mass contributions. In water ρ_s / ρ_f is the specific gravity, s.g., and the mass ratio takes the form

$$m_r = \frac{\pi}{4}(s.g. + C_a) \quad (1.19)$$

To derive the third form of S_u requires that we explicitly evaluate the modal mass M_n . This is done here for two useful cases: i). the spring-mounted rigid cylinder for which the mode shape is $\psi(x)=1.0$, and ii). the flexible cylinder with pinned ends for which the mode shape for mode n is given by

$$\psi_n(x) = \sin\left(\frac{n\pi x}{L}\right) \quad (1.20)$$

In both cases the mode shapes are normalized so that the maximum value is 1.0. The modal mass for each of the two cases may be obtained from:

$$M_n = \int_0^L m_t(x) \psi_n^2(x) dx \quad (1.21)$$

Using equation (1.21), the modal mass, M_n , may be computed providing the added mass per unit length is known, which it is in uniform flows but is not very well known in sheared flows. It is assumed that the total mass per unit length, $\overline{m_t}$, can be represented by its spatial average, $\overline{m_t}$. For a cylinder with uniform structural properties this is equivalent to using an average added mass coefficient to represent added mass on the whole cylinder, which is assumed to be acceptable for the purposes required in this paper.

This in turn leads to an alternative formulation for the mass ratio, as given in equation (1.19).

$$m_r = \frac{\pi}{4} \left(\frac{\rho_s}{\rho_f} + \overline{C_a} \right) \quad (1.22)$$

$\overline{C_a}$ is the spatially averaged added mass coefficient.

Therefore, using an average mass per unit length, the modal mass for mode n may be computed using equation (1.21). This yields the following results:

$$M_n = \overline{m_t} L \quad \text{for the rigid cylinder and} \quad (1.23)$$

$$M_n = \overline{m_t} L / 2 \quad \text{for all sinusoidal mode shapes.}$$

Substituting these expressions for M_n into equation (1.17) and using the definition of mass ratio in equation (1.18), leads to the third useful form for S_u , which is mode shape dependent. For the two mode shapes considered here:

$$S_u = 4\pi^2 S_t^2 m_r \zeta_n \frac{L}{L_{in}} \quad \text{--sinusoidal modes} \quad (1.24)$$

$$S_u = 8\pi^2 S_t^2 m_r \zeta_n \frac{L}{L_{in}} \quad \text{--rigid cylinder mode} \quad (1.25)$$

For uniform flows L/L_{in} reduces to 1.0 and equation (1.25) reduces to the expression frequently cited by Griffin[1982] as the parameter ζ_s / μ or S_G .

$$S_u = \frac{\zeta_s}{\mu} = \frac{8\pi^2 S_t^2 m_e}{\rho_f D^2} \zeta_n, \quad (1.26)$$

$$\text{where } \frac{1}{\mu} = 8\pi^2 S_t^2 \frac{m_e}{\rho_f D^2}$$

The above equation (1.26) is valid only for a uniform, spring-supported, rigid cylinder in a uniform flow. Under these conditions Griffin's m_e and the average total mass per unit length, $\overline{m_t}$, are the same. Iwan and Blevins, 1974, used a parameter called the reduced damping, δ_r , defined as,

$$\delta_r = \frac{2m}{\rho_f D^2} 2\pi \zeta_s. \quad (1.27)$$

This group is also commonly referred to as the Scruton number from [Scruton, 1963]. From this early form the others including S_u have evolved. This form could not deal with sheared flows, partial length power-in regions or hydrodynamic sources of damping. It also did not account for the effect of mode shape on modal mass and damping.

AN ASSESSMENT OF GRIFFIN'S USE OF THE PARAMETER S_G

Griffin attempted to apply equation (1.26) to cylinders with many different mode shapes in uniform flows. He was only partly successful. First, his formulation did not account for the effect mode shape had on modal mass, as required by (1.21). Secondly, he attempted to normalize response amplitudes by means of a factor $I_i^{1/2}$, which is a consequence of assuming a wake oscillator formulation of the hydrodynamic excitation. These issues are examined below. The wake oscillator model does not adequately account for real-world variations in lift due to such things as Re, turbulence and roughness.

First, consider the effective mass. It is defined in [Griffin, 1982] as

$$m_e = \frac{\int_0^L m(x) y^2(x) dx}{\int_0^h y^2(x) dx}. \quad (1.28)$$

In this formulation $y(x)$ is a mode shape, $m(x)$ is the total mass per unit length, L is the total structure length, h is the portion of the riser in the water. The equation was derived based on the argument that an equivalent structure with a constant mass per unit length, m_e , would have the same vibrational kinetic energy as one with the actual mass per unit length $m(x)$. This result is only true if the lower integral is carried out over the whole length from 0 to L . That is, equation (1.28) would be correct if h were replaced by L . If this is done then the structure with mass per unit length m_e would have the same modal mass, M_n , and the same kinetic energy as the real structure.

The Griffin formulation also does not correctly account for the difference in modal masses introduced by different mode shapes, as illustrated in the differences shown in this paper between the formulations in equations (1.24) and (1.25) for rigid cylinders and ones with sinusoidal mode shapes.

Griffin, 1982, attempted to eliminate the influence on mode shape by plotting a normalized maximum response, Y_{EFF}/D , versus the parameter ζ_s/μ . Y_{EFF}/D was defined in the following way, where Y is the maximum modal response, the equivalent of q_n in this paper.

$$\frac{Y_{EFF}}{D} = \frac{Y}{D} \frac{I_i^{\frac{1}{2}}}{\psi(x)_{i,max}}, \text{ where} \quad (1.29)$$

$$I_i = \frac{\int_0^L \psi(x)_i^4 dx}{\int_0^L \psi(x)_i^2 dx} \quad (1.30)$$

In the case of sinusoidal mode shapes the factor I_i is $\frac{3}{4}$ and $I_i^{\frac{1}{2}} = 0.866$. Using the normalization that the maximum mode shape amplitude is 1.0, then for sine wave mode shapes:

$$\frac{Y_{EFF}}{D} = \frac{Y}{D} \frac{I_i^{\frac{1}{2}}}{D} = 0.866 \frac{Y}{D} \quad (1.31)$$

Griffin plotted Y_{EFF}/D versus ζ_s/μ for structures with a wide variety of mode shapes. The results were encouraging, but had wide scatter in the data, which was in part due to the attempt to account for too many mode shapes in one figure with the normalization factor $I_i^{\frac{1}{2}}$.

The application of this factor was independently published by [Iwan, 1975] and by [Skop and Griffin in 1975]. Figure 1 is a modified reproduction of Griffin's figure. The modification by the author is the addition of lines of constant lift coefficient, which will be described in the next section.

Griffin's laudable attempt to find a single parameter, which would collapse a wide variety of response data into one understandable curve has intrigued this author for twenty-five years. Griffin was able to collect a wide variety of response data onto one curve, but with such large scatter as to make the user uncomfortable with its reliability. The conclusion reached in this paper is that Griffin had the right idea, but tried to explain too wide a variety of data with the correction factor, $I_i^{\frac{1}{2}}$. Experimental data, in general have many additional factors which contribute to scatter. These include Reynolds' number, turbulence, roughness and reduced velocity.

The approach recommended here is to plot together only response data from structures of one mode shape type, such as sinusoidal, on one plot of S_u versus A/D . This reduces the sources of scatter in the response data to a more easily identified and manageable collection.

THE RELATIONSHIP BETWEEN LIFT COEFFICIENT AND THE PARAMETER S_u

Equation (1.10) relates the modal response amplitude q_n to S_u .

$$\frac{q_n}{D} = \frac{\langle C_{L,n} \rangle}{2} \frac{\rho U^2 L_{in}}{R_n \omega_n} = \frac{\langle C_{L,n} \rangle}{2 S_u}$$

Modal analysis provides a simple means of expressing the vibration amplitude at all points on the real structure in terms of the modal amplitude q_n and the mode shape. For example, the transverse vibration of a flexible cylinder, $w_n(x)$, is given by

$$w_n(x) = q_n \psi_n(x) \quad (1.32)$$

If one uses the normalization that the maximum amplitude of the mode shape is 1.0, then the peak response amplitude of the cylinder, A , is equal to the modal amplitude q_n . Therefore

$$\frac{A}{D} = \frac{q_n}{D} \quad (1.33)$$

Using this definition and solving equation (1.10) for $\langle C_{L,n} \rangle$ leads to the equation of a hyperbola:

$$\langle C_{L,n} \rangle = 2 S_u \frac{A}{D} \quad (1.34)$$

On a linear plot of S_u versus A/D lines of constant, mean, modal lift coefficient are hyperbolas, which form straight lines on a log-log scale. Griffin's plot shown in Figure 1 is such a log-log plot with the lines of constant $\langle C_{L,n} \rangle$ added by this author for the case of spring-mounted rigid cylinders. Other mode shapes would have slightly displaced lift coefficient lines due to different values of the factor $I_i^{\frac{1}{2}}$. For data points on the plot it is possible to deduce the approximate average lift coefficient that was at work in order for dynamic equilibrium to be satisfied in equation (1.9)

By plotting response data on such a curve, and plotting experimentally determined (S_u , A/D) data points, it is possible to infer the mean modal lift coefficient, $\langle C_{L,n} \rangle$. For example, at very low values of S_G in the Griffin plot, the curve flattens out at $2 * Y_{EFF}/D$ values of 2.0 to 4.0. This is a consequence of the limit cycle behavior of VIV at large response amplitudes. Peak amplitudes are self-limited, because the mean lift coefficient drops to very low values. Typical values of $\langle C_{L,n} \rangle$ in the limit cycle region are less than 0.05.

At high values of S_g the Griffin plot takes on the slope of the lines of constant average lift coefficient. Typical values of $\langle C_{L,n} \rangle$ in this region are 0.4 to 0.8. In this region the structure is extracting the maximum possible energy from the fluid. The response is limited because the damping is large enough to dissipate all of the energy that can be extracted from the fluid, without requiring that limit cycle effects diminish the local lift coefficient. Plots of the more general parameter S_u versus A/D for one type of mode shape may also include curves of constant lift coefficient.

It is important to keep in mind that $\langle C_{L,n} \rangle$ comes from equation (1.6). It is the average of the lift coefficient times the mode shape. The average is computed over the length of the power-in region. This means that at locations where the mode shape is large, the lift coefficient may be zero or even negative, while small amplitude regions may have quite large local lift coefficients. It is recommended that all, available, sinusoidal mode shape, VIV data be assembled on graphs such as these. By limiting the data to structures with one type of mode shape, many uncontrolled variables will be removed from the problem. Examples are shown next.

THE APPLICATION OF S_u TO RISER RESPONSE IN SHEARED FLOW

Equation (1.10) captures the four principal unknowns required for VIV response prediction. For a specified shear profile these unknowns are the length and location of the power-in region, the modal damping and the modal lift coefficient. Of these the one least understood is the lift coefficient. Therefore, lift coefficient is left as a free parameter to be inferred from experiments in which the response is measured.

This leaves three parameters to be estimated for inclusion in the parameter S_u . The first two are location and length of the power-in region. With each response measurement the response frequency and by inference the excitation frequency is also determined. By selecting upper and lower bounds to the reduced velocity and making use of the measured response frequency, the upper and lower velocity limits of the power-in range may be estimated. The fraction of the riser length, which has flow velocities between these two limits determines the length of the power-in region, L_{in} .

The location of the power-in zone is equivalent to picking the mean power-in flow velocity, U_n , which depends on the average reduced velocity in the power-in zone. The average reduced velocity is equivalent to an effective Strouhal number. The upper and lower bounds of the reduced velocity may be dependent on Reynolds number and roughness, but not added mass. Appropriate values must be extracted from experiments. In the next section a numerical experiment is conducted which illustrates the effect of the location and length of the power-in region.

The third unknown property is the damping. Damping may come from structural and hydrodynamic sources. In sheared flows the hydrodynamic contribution is often dominant and must be estimated from empirical formulae, such as described in [Vikestad, 2000]. An example is shown later in the presentation of experimental data.

The Response of an example riser in a linear sheared flow as a function of power-in length

A typical vertical production riser is used to illustrate the use of the parameter S_u in presenting response data. The example, water-filled, steel riser has the following properties:

Length = 1021 m(3350 feet)
 Outside Diameter = 0.340 m(13.375 inches)
 Inside Diameter = 0.315 m(12.415 inches)
 Top Tension = 2.945 MN(662,000 lbs)
 Bottom Tension = 1.334 MN(300,000 lbs)

Figure 2 shows several linear sheared profiles and two uniform flow profiles. The linear profiles have a minimum velocity of 0.0 m/s and maxima ranging from .152 m/s(0.5 ft/s) to 1.83 m/s(6.0 ft/s) in increments of 0.152 m/s(0.5 ft/s).

The program SHEAR7 was used to estimate the response of the dominant mode of the production riser for six different values of reduced velocity bandwidth, which is defined in the next equation. SHEAR7 specifies the location of the power-in region for each mode by means of a Reynolds number dependent Strouhal number which varies linearly from 0.17 at a Reynolds number of 20K to 0.24 at 90K. It remains at .24 above 90K. The center of the power-in region for each possible excited mode is located in the profile at a reduced velocity of $1/S_t$. The upper and lower limits of the power-in zone are located at values of V_R given by

$$V_{R,upper} = \frac{1}{S_t}(1 + \Delta V_r / 2)$$

$$V_{R,lower} = \frac{1}{S_t}(1 - \Delta V_r / 2), \quad (1.35)$$

Where $\Delta V_R \equiv$ bandwidth

The reduced velocity bandwidths were varied from 0.1 to 0.6. Figure 3 is the plot of the predicted response RMS A/D versus the parameter S_u . The values of power-in length, L_{in} , modal mass and modal damping, necessary for the computation of S_u were taken directly from the output files generated by SHEAR7.

SHEAR7 is a mode superposition program, which iteratively determines the lift coefficient, damping and response A/D which satisfy dynamic equilibrium as required by equation (1.10). The damping and lift coefficient models used in SHEAR7 are dependent on A/D and Reynolds number. The hydrodynamic damping is also reduced velocity dependent. SHEAR7 may be set so that it finds the dominant mode out of all possible responding modes and then computes the response for only that mode. This 'single mode' setting was used for this illustration.

In Figure 3 a unique symbol is used for each bandwidth. Response is computed for all twelve sheared profiles for each bandwidth setting. As expected, the response increases with the power-in length, which is determined by the bandwidth. In the figure, the minimum response for each bandwidth setting usually corresponds to the minimum velocity profile. Response increases with the maximum current in the profile. For each group of points sharing the same bandwidth, there is a maximum and minimum dominant mode number corresponding to the maximum and minimum peak flow velocity. These modes

varied from the 29th mode at the peak flow speed of 1.82 m/s down to modes 1 or 2 at the minimum flow speed. The mode number range for each bandwidth is indicated in parentheses in the legend title.

At the same bandwidth one would expect the value of S_u to decrease with higher RMS A/D. This does not happen in Figure 3, because the hydrodynamic damping model used in SHEAR7 increases with A/D. This leads to the unexpected variation in S_u . It is also a good reminder that the inherent non-linearity of the VIV phenomena will cause significant variation of A/D values, even at exactly the same value of S_u . The parameter does not account for the non-linear behavior of VIV. Whereas, SHEAR7 does include the non-linear modelling of C_L and damping.

At the far left of Figure 3 there are two data points at an RMS A/D value of 0.87. These are the positions of the data points for the two uniform flow profiles. These RMS values correspond to peak A/D values of 1.23. In uniform flow cases the bandwidth is irrelevant, because only a tiny bandwidth is required to span the entire profile. These two points used a reduced velocity bandwidth of 0.1.

At the far right of Figure 3 are two renegade points. These are the result of normal variation in the location of power-in regions, which occasionally results in a dominant mode having a part of the allowable bandwidth falling outside of the current profile. This results in reduced response and increased damping. These are mode 1 dominated cases in very low current velocity. Figure 3 also has several hyperbolas plotted. These correspond to the mean modal lift coefficient $\langle C_{L,n} \rangle$. It is possible to read off the plot that the mean modal lift coefficient for the two uniform flow cases was approximately 0.02, indicating that the two cases shown were very much limit cycle controlled. In contrast most of the data points for the sheared flow cases fall between mean modal lift coefficients of 0.2 and 0.4.

This numerical example has demonstrated the sensitivity of the parameter S_u to variations in the key variables that define it. In real sheared flow experiments the length of the power-in region is rarely known. Figure 3 provides some insight as to the expected behavior. In the next section data from an unusual experiment is presented in which the length and location of the power-in region was known.

THE RESPONSE OF FLEXIBLE CYLINDERS IN UNIFORM FLOW WITH REGIONS OF STILL WATER

Description of experiments In 1985 Demos Tsahalis of Shell Development Company conducted an interesting set of tests on a towed horizontal cylinder, 13.88 meters (44.21 feet) in length in a test basin [Tsahalis, 1985]. The tube had a specific gravity of 2.49, including contents. The tube was made of 304 A269 stainless steel tubing (OD=0.0381 m (1.5 inches)), ID=0.0339 (1.334 inches)). Wires and accelerometers were inside of a Tygon tube, which was pulled into the stainless tube. The cylinder had pinned ends and sinusoidal mode shapes. Bi-axial

accelerometers were used to measure response at positions L/8, L/4, L/2, 5L/8, and 5L/6.

The unique feature of this experiment was that a shroud was constructed which surrounded a portion of the cylinder. The shroud traveled with the cylinder and created a still water region around the cylinder. The length of the cylinder protected by the shroud was varied in seven steps, covering 0, 12.5%, 25%, 37.5%, 50%, 62.5%, and 75% of the model. Towing velocity was varied from 0.101 m/s to 1.83 m/s (0.33 to 6.0 ft/s) in steps of 0.101 m/s. These speeds corresponded to a Reynolds' number range of 4200 to 89000. Water temperature varied from 75 to 88 degrees Fahrenheit (24 to 31 degrees Centigrade) First through third mode of vibration was observed for cross-flow vibration and first through fifth mode was observed in-line.

The tension was not measured during experiments, but was determined to be approximately 1544 pounds, in still water. The measured natural frequencies in still water were for modes 1, 2, 3, and 5: 1.80, 3.40, 5.80, and 12.15 Hz with a variation of approximately plus or minus 3% from test to test.

Lock-in behavior was observed primarily for the second and third modes in the direction transverse to the flow. Second mode experienced a range of reduced velocity in the tests, which completely covered its lock-in region. Second mode lock-in often initiated at around 0.71 m/s and ceased above 1.12 m/s. The 1985 report does not report tension, but it does tabulate the observed vibration frequency and the flow speed. It is possible to compute a reduced velocity range inserting the observed vibration frequency and the towing velocity into the following equation.

$$V_r = \frac{U}{f_{v,2} D} \quad (1.36)$$

where $f_{v,2}$ is the observed 2nd mode vibration frequency.

Data reduction The procedure used to estimate response amplitude was described in the Tsahalis report. The accelerometer time series data were Fourier transformed. Each Fourier frequency component was double integrated in the frequency domain. Then the final displacement time history was obtained by an inverse Fourier transform of the integrated Fourier components. Modal participation was determined by curve fitting the responses at the five accelerometer locations. It was not possible to check the procedure as described in the report, but the data taken from tables in the report seem quite reasonable.

Since second mode was the only mode, which was tested over its full lock-in range, only second mode data is presented in this paper. Second mode lock-in events were identified and plotted on a plot of S_u versus A/D. Equation (1.15) was used to compute S_u . This required computation of the total modal damping and the modal mass for the appropriate mode. The modal mass contribution was simply determined using equation (1.23), where the average added mass coefficient was set at 0.0.

$$\overline{m}_t = \frac{\pi}{4} \rho_f D^2 (s.g. + \overline{C}_a) = \frac{\pi}{4} \rho_s D^2 \quad (1.37)$$

From equation (1.23) we can compute the modal mass as,

$$M_n = \overline{m_t} L / 2, \text{ where } \overline{m_t} = \overline{m_t} \quad (1.38)$$

Given that the specific gravity of the cylinder was 2.49, the modal mass for all tests was approximately 19.12 kg (1.31 slugs). Of course the actual added mass varied with reduced velocity and shroud length, but for the purposes of computing representative values of S_u the value given above is more than adequate.

Estimation of modal damping

The estimation of modal damping required an hydrodynamic damping estimate for a vibrating cylinder in still water. The hydrodynamic damping was then added to the structural damping, which was measured in air at 0.3% of critical. Still water hydrodynamic damping for vibrating cylinders is quite well documented experimentally. Vikestad et al, 2000, provide a recent set of measurements and previous references. A curve fit to measured still water damping, as a function of A/D and vibration Reynolds number is used in the VIV response prediction program SHEAR7. In this model the hydrodynamic damping force per unit length per unit velocity for a cylinder in still water is given by

$$r_{sw}(x) = \frac{\omega_n \rho_f \pi D^2}{2} \left[\frac{2\sqrt{2}}{\sqrt{R_{e,\omega}}} + 0.2 \left(\frac{A}{D} \psi_n(x) \right)^2 \right], \quad (1.39)$$

$$\text{Where, } R_{e,\omega} = \frac{\omega_n D^2}{\nu}$$

The modal hydrodynamic damping is obtained from the integral given in equation (1.7)

$$R_{h,n} = \int_{L_{out}} r_n(x) \psi_n^2(x) dx \quad (1.7)$$

In this case L_{out} is the length covered by the shroud. This is the length over which the modal damping integral is conducted. The remainder of the cylinder is in uniform flow and is the power-in region for whatever mode is resonantly excited by the flow. Once $R_{h,n}$ is found then the hydrodynamic damping ratio may be obtained from equation (1.2) and added to the structural damping ratio to obtain the total damping ratio.

$$\zeta_{h,n} = \frac{R_{h,n}}{2\omega_n M_n} \quad (1.40)$$

$$\zeta_{t,n} = \zeta_{s,n} + \zeta_{h,n} \text{ the total modal damping ratio.} \quad (1.41)$$

The second form of S_u from equation (1.15) was used to compute values for plotting

$$S_u = \frac{8\pi^2 M_n \zeta_n}{\rho_f D^2 L_{in} V_R^2} \quad (1.42)$$

Equation (1.38) provides that the modal mass for this case is given by $M_n = \overline{m_t} L / 2$, which yields a more convenient form of equation (1.42)

$$S_u = \frac{4\pi^2 \overline{m_t} \zeta_n L}{\rho_f D^2 V_R^2 L_{in}} \quad (1.43)$$

This further reduces to

$$S_u = \frac{\pi^3 \zeta_n L}{V_R^2 L_{in}} (s.g.) \quad (1.44)$$

Where we have made use of equation (1.37) with C_a set to zero. From the Tsahalis report all of the components of equation (1.44) are known except the still water damping which may be computed from the experimental conditions using equations (1.7) and (1.39).

Figure 4 is a plot of the response A/D versus S_u . There are three points, which have very high A/D values at large values of S_u . It was not possible to check the original time series, but the author suspects that data processing errors may have been responsible. In particular, low frequency noise in the data might have been exaggerated in the process of double integration.

Although the data in the reports had limitations, which were aggravated by the fact that the original times series no longer existed, there is much to be learned from this experiment. In particular this is a rare opportunity to have a single cylinder with constant properties tested over a reasonably broad range of hydrodynamic damping values. Since the hydrodynamic damping was still water damping from water trapped inside of the shroud, the damping can be computed with reasonable accuracy. Secondly, the power-in region length is accurately known and it was possible to isolate single mode lock-in cases and plot response versus S_u and V_R .

Figure 5 is a plot of response versus reduced velocity based on the vibration frequency. The second mode lock-in range varied from reduced velocities of approximately 5 to 8. The center value was 6.5, which corresponds to a Strouhal number of 0.154. The data used to plot Figures 4 and 5 are summarized in Tables 1A and 1B.

SHEAR7 was also used to compute the response to the same flow conditions. The SHEAR7 predictions using single mode settings and $S_t = 0.154$ are also plotted in Figure 4. With the exception of the three questionable data points SHEAR7 is conservative in all but the 100% exposure length cases, where the prediction is a small amount low. The 100% exposure length case is very sensitive to the limit cycle modeling used in the program. For these cases the SHEAR7 V4.2 model used a lift coefficient relationship which became negative above an A/D of 1.1.

CONCLUSIONS AND RECOMMENDATIONS

The parameter, S_u , has been proposed which is useful in organizing uniform and sheared flow response data according to power-in length, damping, and flow velocity. Once plotted the parameter may be interpreted in terms of the average modal lift coefficient.

The next steps in the application of this parameter are to gather a wide variety of sinusoidal mode shape response data at various combinations of Reynolds number and roughness. With response versus S_u plots for many conditions, engineers will have a standard for comparison of simple estimates and a powerful tool for calibrating response prediction programs.

Future areas of research in the development of this parameter are the establishment of protocols for dealing with multi-mode response data, response at very high mode numbers and response under unsteady flow conditions.

ACKNOWLEDGMENTS

The author would like to thank Shell Global Solutions for granting permission to publish the data presented in this paper. This research was sponsored by a consortium of oil industry companies and by the Office of Naval Research, Ocean Engineering division, Code 321; Award number N00014-95-1-0545.

REFERENCES

Griffin, O. M., & Ramberg, S.E., 1982, "Some Recent Studies of Vortex Shedding with Application to Marine Tubulars and Risers", ASME J. of Energy Resources Technology, Vol. 104, pp. 2-13.

Griffin, O., M., 1984, "Vibrations and Flow-Induced Forces Caused by Vortex Shedding", Symposium on flow-Induced Vibration, Volume 1, ASME Winter Annual Meeting.

Iwan, W.,D., & Blevins, R. D., 1974, J. of Applied Mechanics, "A Model for Vortex Induced Oscillation of Structures", Vol. 41(Series E #3), pp. 581-586, Sept. 1974.

Iwan, W.,D., 1975, "The Vortex Induced Oscillation of Elastic Structural Elements", J. of Engineering for Industry, ASME, Vol. 97, pp. 1378-1382.

Scruton, C. "On the Wind-Excited Oscillations of Stacks, Towers and Masts", Proc. of the Wind Effects on Buildings and Structures Conference, NPL, Teddington, England, June 1963.

Skop & Griffin, 1975, "On a Theory for the Vortex-Excited Oscillations of Flexible Cylindrical Structures", J. of Sound and Vibration, Vol 41(3), pp. 263-274.

Vandiver, J. K., 1985, "Prediction of Lockin Vibration on Flexible Cylinders in Sheared Flow," Proceedings of the 1985 Offshore Technology Conference, Paper No. 5006, Houston, May 1985.

Vandiver, 2000, "Predicting Lock-in on Drilling Risers in Sheared Flows", Proceedings of the 7th International Conference on Flow-Induced Vibration FIV2000, Lucerne, Switzerland, June 19-22, 2000, Ziada and Staubli (eds).

Tsahalis, D.,T., 1985, "Experimental Study of the Vortex Induced Vibrations of a Long Model Riser Exposed to Uniform and Non-uniform Steady Flow", Houston, Texas, Westhollow Research Center report WRC 47-85 & 55-85.

Vandiver, J.K., Lee, L., 2002, SHEAR7 User Guide, MIT, Cambridge, MA, USA.

Vikestad, K., Larsen, C.M., Vandiver, J.K., 2000, "Norwegian Deepwater Program: Damping of Vortex-Induced - Vibrations", Proc. 2000 Offshore Technology Conference, Paper 11998.

Table 1A. Tabulated data from Tsahalis							
U(ft/s)	f(Hz)	Max A/D	Vr	f(Hz)	Max A/D	Vr	
25 % Exposure length, Run M				Run N			
2.00	3.00	0.37	5.33	3.08	0.20	5.19	
2.33	3.31	0.38	5.63	3.19	0.49	5.84	
2.67	3.49	0.18	6.12	3.44	0.38	6.21	
3.00	3.60	0.13	6.67	3.56	0.24	6.74	
37.5% Exposure Length, Run P				Run Q			
2.00	2.81	0.29	5.69	2.91	0.22	5.50	
2.33	2.96	0.47	6.30	3.01	0.45	6.19	
2.67	3.07	0.67	6.96	3.17	0.63	6.74	
3.00	3.16	0.85	7.59	3.26	0.82	7.36	
3.33	3.58	1.29	7.44	3.60	1.29	7.40	
3.66	3.82	0.38	7.69	3.72	1.29	7.89	
3.99	4.22	0.22	7.58	3.99	0.40	8.02	
50% Exposure Length, Run R				Run S			
2.00	2.87	0.29	5.57	2.81	0.32	5.69	
2.33	2.97	0.43	6.28	2.93	0.47	6.36	
2.67	3.10	0.52	6.89	3.09	0.56	6.91	
3.00	3.20	0.64	7.50	3.19	0.66	7.52	
3.33	3.38	0.82	7.88	3.49	1.17	7.63	
3.66	3.99	0.51	7.36	4.12	0.51	7.13	
3.99	4.51	0.56	7.10	4.40	0.62	7.27	
62.5% Exposure Length, Run T				Run U			
2.00	2.81	0.33	5.69	2.90	0.21	5.52	
2.33	2.98	0.40	6.26	2.99	0.51	6.23	
2.67	3.25	0.21	6.57	3.20	0.32	6.68	
3.00	3.40	0.39	7.06	3.38	0.35	7.10	
3.33	3.57	0.49	7.46	3.50	0.44	7.61	
3.66	3.79	0.93	7.75				
3.99	4.53	0.31	7.06				

Table 1B. Tabulated data from Tsalhis

U(ft/s)	f(Hz)	Max A/D	Vr	f(Hz)	Max A/D	Vr
75% Exposure Length, Run W				Run X		
2.00	2.68	0.32	5.97	2.60	0.37	6.15
2.33	2.98	0.67	6.26	2.98	0.62	6.26
2.67	3.11	0.87	6.87	3.10	0.85	6.89
3.00	3.46	0.30	6.94	3.47	0.25	6.92
3.33	3.58	0.44	7.44	3.70	0.55	7.20
3.66						
3.99						
87.5% Exposure Length, Run Y				Run Z		
2.33	2.90	0.62	6.43		0.54	6.85
2.67	3.27	0.68	6.53	3.25	0.74	6.57
3.00	3.50	0.81	6.86	3.50	0.85	6.86
3.33	3.71	0.91	7.18	3.72	0.94	7.16
3.66	3.92	1.05	7.49	4.01	1.10	7.32
3.99	4.02	1.03	7.96	4.53	0.44	7.06
100% Exposure Length, Run A				Run B		
2.33	2.91	0.48	6.41	2.87	0.42	6.49
2.67	3.30	0.88	6.47	3.18	0.82	6.72
3.00	3.50	0.76	6.86	3.48	0.75	6.90
3.33	3.73	1.01	7.14	3.70	0.78	7.20
3.66	3.98	1.06	7.38	3.92	1.24	7.49
3.99	4.10	1.43	7.80	4.08	1.43	7.84
100% Exposure Length, Run C						
2.33	2.76	0.44	6.75			
2.67	3.21	0.90	6.65			
3.00	3.50	0.73	6.86			
3.33	3.71	0.99	7.18			
3.66	3.93	1.15	7.47			

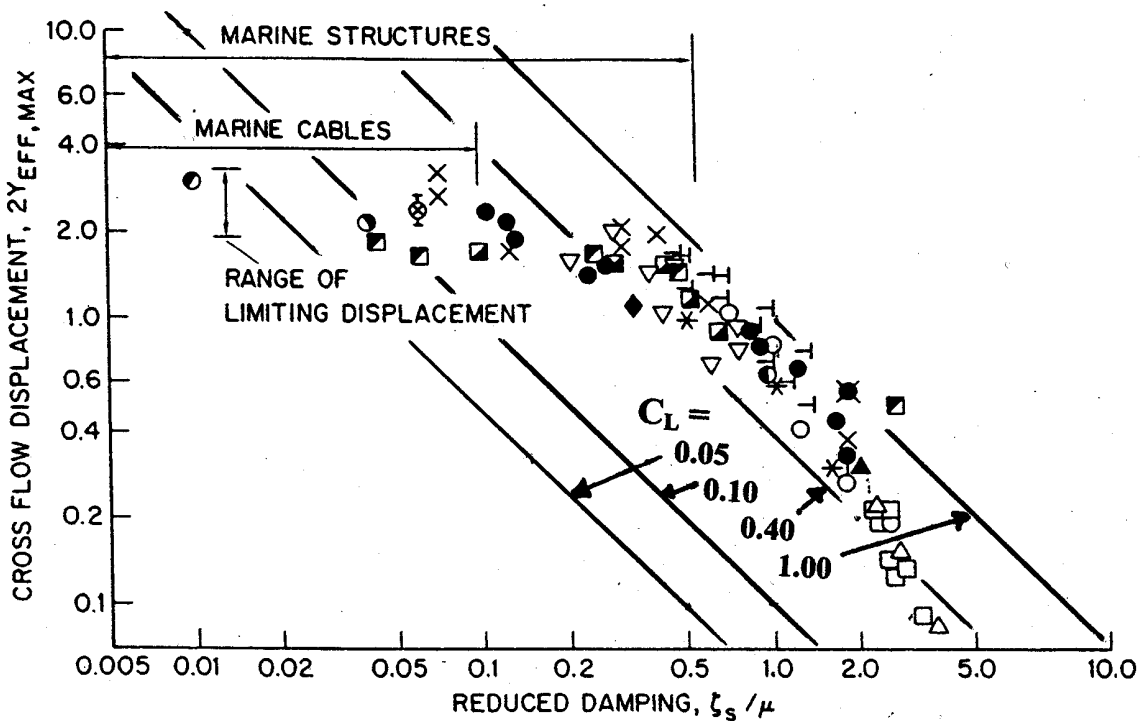


Figure 1. Response versus ζ_s / μ from [Griffin, 1982], Lines of constant C_L added by Vandiver

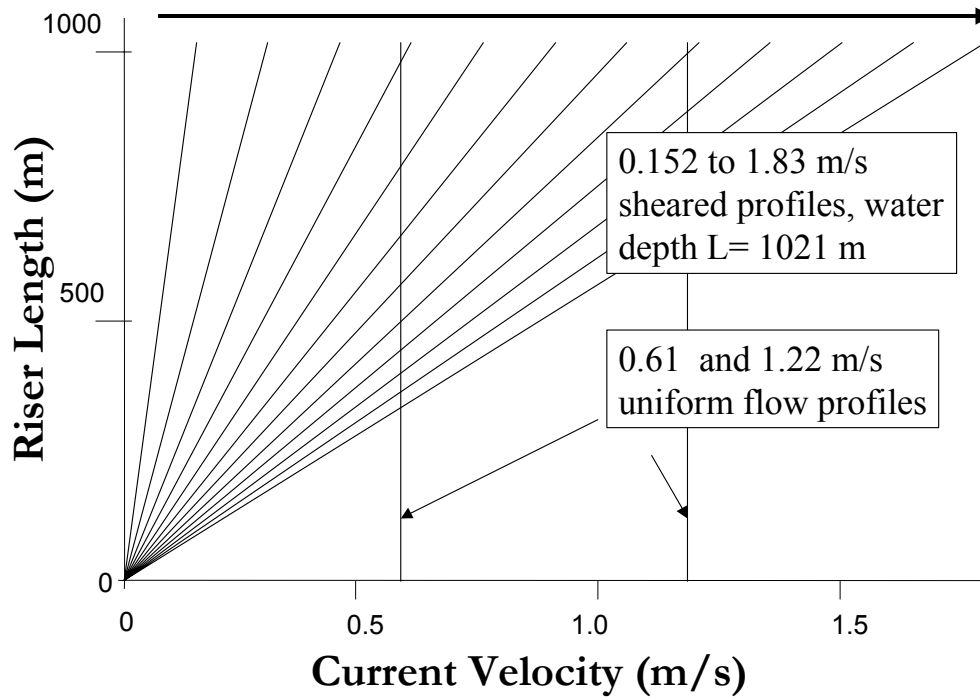


Figure 2. Current profiles used in SHEAR7 predictions of response.

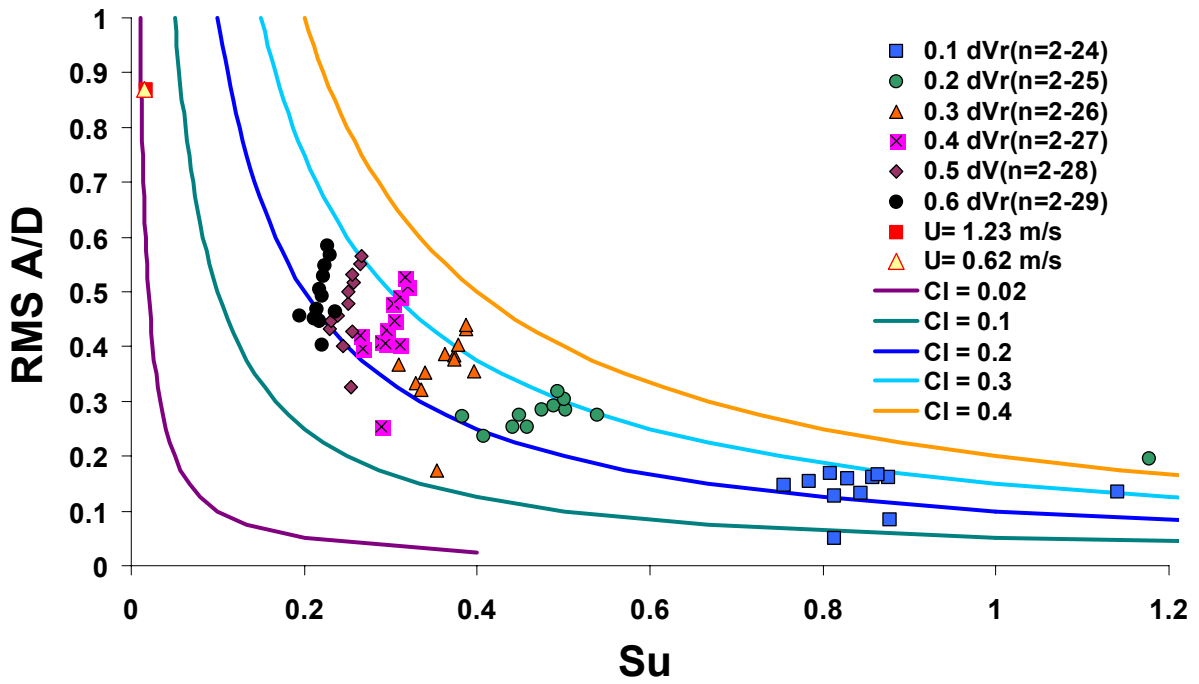


Figure 3. S_u and versus RMS A/D from SHEAR7 for various ΔV_R , $\langle C_L \rangle$ are the hyperbolas

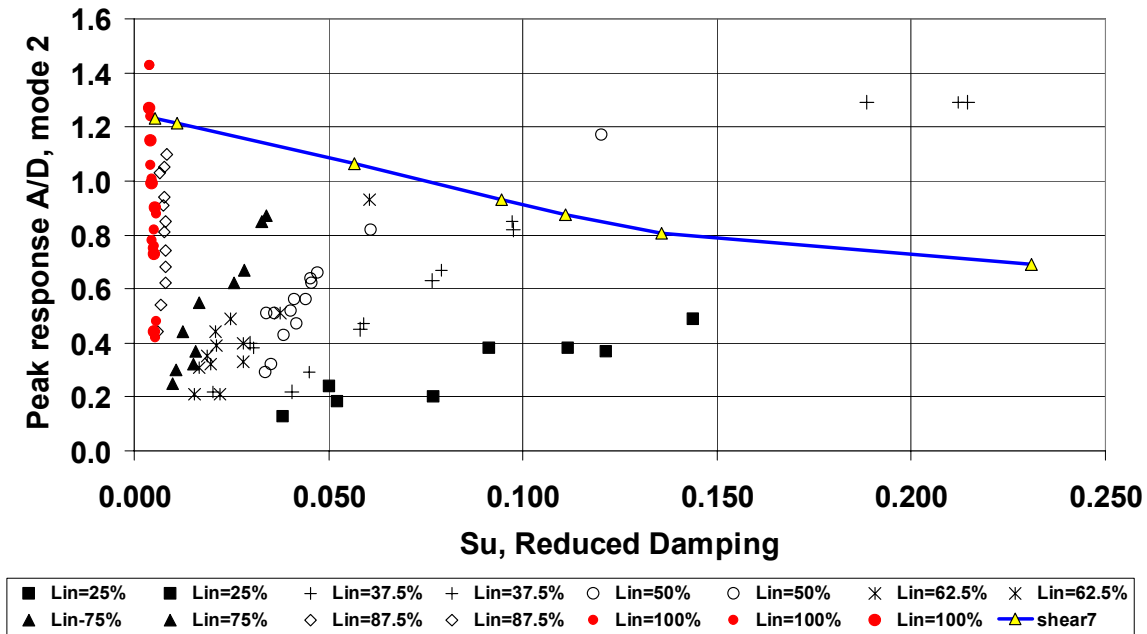


Figure 4. S_u vs. 2nd mode peak A/D as a function of exposure length. Data from Tsahalís, 1985. SHEAR7 prediction shown for comparison.

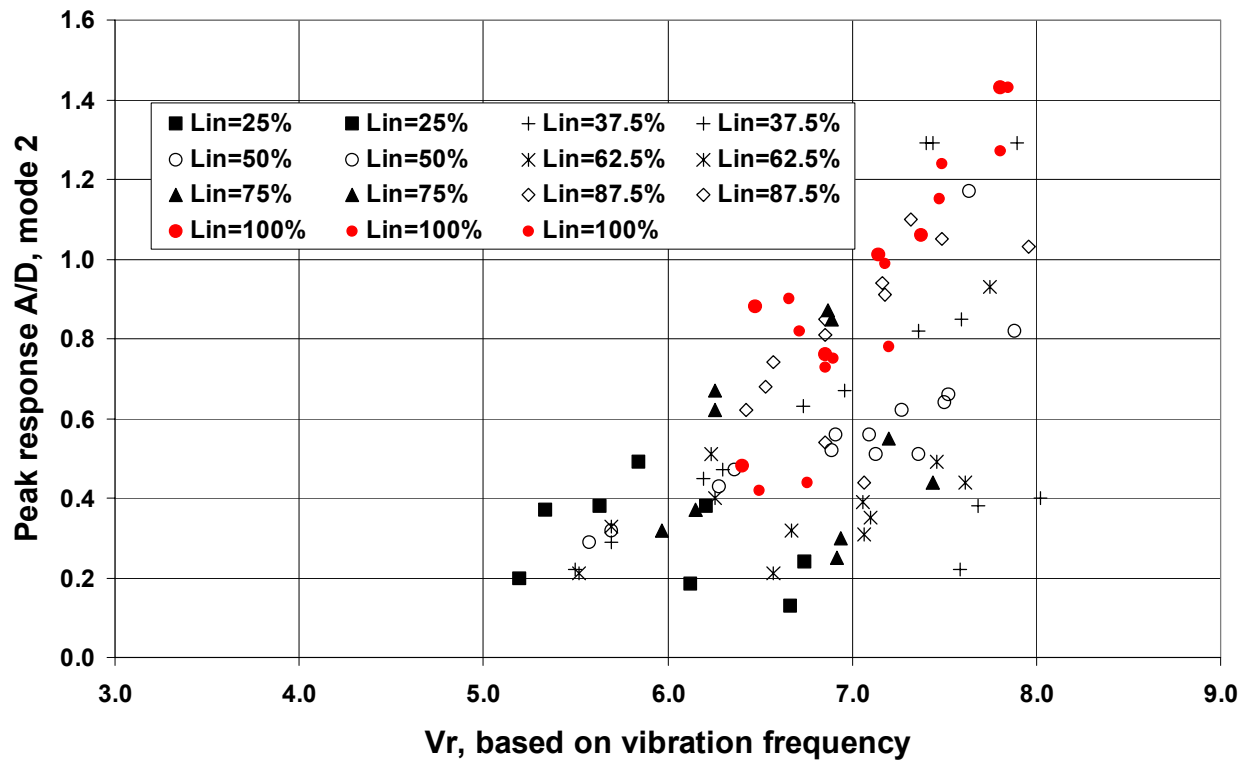


Figure 5. Peak response A/D versus reduced velocity, V_R . Data from [Tsahalis, 1985].